Force generated by a swelling elastomer subject to constraint

Shengqiang Cai,[1] Yucun Lou,[2] Partha Ganguly,[2] Agathe Robisson,[2] and Zhigang Suo[1,a)]
[1]*School of Engineering and Applied Sciences, Harvard University, Cambridge, Massachusetts 02138, USA*
[2]*Schlumberger-Doll Research, One Hampshire Street, Cambridge, Massachusetts 02139, USA*

(Received 26 January 2010; accepted 16 April 2010; published online 26 May 2010)

When an elastomer imbibes a solvent and swells, a force is generated if the elastomer is constrained by a hard material. The magnitude of the force depends on the geometry of the constraint, as well as on the chemistry of the elastomer and solvent. This paper models an elastomer crosslinked on the exterior surface of a metallic tubing. The elastomer then imbibes a solvent and swells. After the swollen elastomer touches the wall of the borehole, a significant amount of time is needed for the solvent in the elastomer to redistribute, building up the sealing pressure to the state of equilibrium. The sealing pressure and the sealing time are calculated in terms of the geometric parameters (i.e., the thickness of the elastomer and the radii of the tubing and borehole), the number of monomers along each polymer chain of the elastomer, and the affinity between the elastomer and the solvent.
 [doi:10.1063/1.3428461]

I. INTRODUCTION

Flexible polymeric chains can be crosslinked by covalent bonds into a three-dimensional network, resulting in an elastomer. The elastomer can imbibe a solvent, a phenomenon that is ubiquitous among animals and plants, and is exploited in creating commercial products such as contact lenses[1] and superabsorbent diapers.[2] Upon imbibing the solvent, the elastomer swells. Furthermore, if the elastomer is constrained by a hard material, the swelling generates a force. Swelling is used by plants to regulate the transport of water,[3] and is being developed for engineering applications, such as self-regulating microfluidics,[4,5] self-healing cements,[6–8] and packers.[9–12] Essential to these applications are the force generated by swelling, and the time needed to build up the force.

The magnitude of the force depends on the geometry of the constraint, as well as on the chemistry of the elastomer and solvent. The time needed to build up the force depends on the diffusivity and on the distance through which the solvent must migrate. To illustrate these issues, this paper models swelling packers used in oilfields.[9–12] Such a packer consists of an elastomer crosslinked around the exterior surface of a metallic tubing, Fig. 1. Once the packer is deployed in a borehole, the elastomer imbibes a solvent (either water or oil, depending on applications), swells to the size of the borehole, and builds up a sealing pressure on the wall of the borehole.

Despite intense experimental efforts to develop the packers to enhance the production of oil, theoretical modeling of packers is lacking. The object of this paper is to calculate the sealing pressure and the sealing time of a swelling packer. Section II presents the governing equations on the basis of a nonlinear field theory of concurrent deformation and migration. Section III calculates the sealing pressure when the network equilibrates with the solvent. Emphasis is placed on the effects of the number of monomers along each polymer chain of the elastomer, the affinity between the elastomer and the solvent, and various geometric parameters (i.e., the thickness of the elastomer and the radii of the tubing and borehole). Section IV calculates the time needed to approach the state of equilibrium. After the elastomer swells to the size of the borehole, substantial time is needed for the solvent molecules in the elastomer to redistribute and build up the sealing pressure.

II. GOVERNING EQUATIONS FOR CONCURRENT DEFORMATION AND MIGRATION

Figure 1 illustrates a layer of an elastomer, length L, crosslinked around the exterior surface of a metallic tubing of radius A. For the packer to be readily inserted into a borehole of radius B, the gap between the tubing and the bore-

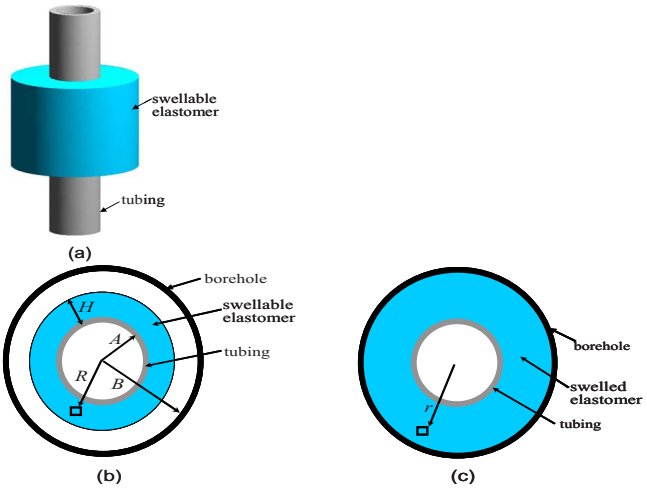

FIG. 1. (Color online) (a) A packer consists of an elastomer crosslinked around the exterior surface of a metallic tubing. (b) When the elastomer is dry, the radius of the packer is smaller than that of the borehole. (c) As the solvent migrates into the elastomer, the elastomer swells to the size of the borehole.

a)Electronic mail: suo@seas.harvard.edu.

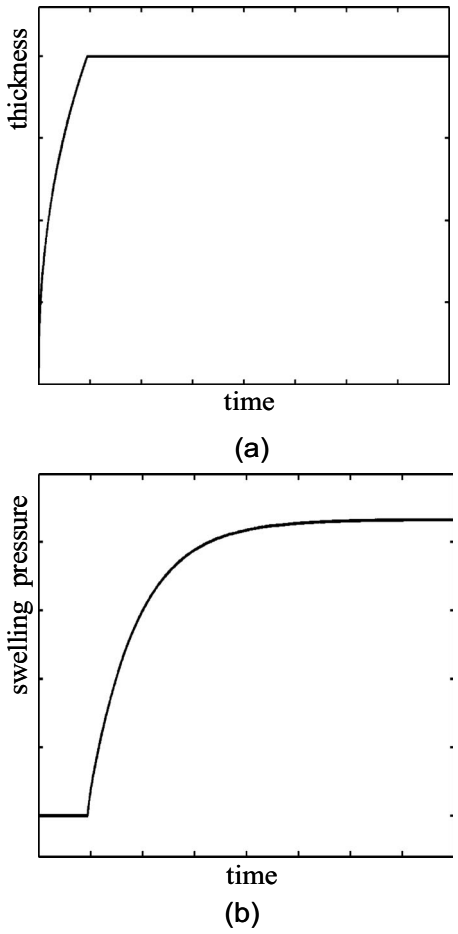

FIG. 2. (a) As the elastomer imbibes the solvent, the thickness of the elastomer increases from H to $B-A$. (b) Before swelling to the size of the borehole, the elastomer exerts no pressure. After the elastomer touches the wall of the borehole, the solvent molecules inside the elastomer redistribute, and the pressure builds up, approaching a state of equilibrium.

hole, $B-A$, should be larger than the thickness of the dry elastomer, H. As the solvent migrates into the elastomer, the elastomer swells and closes the gap. Figure 2 sketches the thickness of the swelling elastomer as a function of time. Also sketched is the pressure exerted by the elastomer on the wall of the borehole as a function of time. Prior to touching the wall of the borehole, the elastomer exerts no pressure on the borehole. Afterwards, the solvent molecules in the elastomer redistribute, and the sealing pressure builds up. The sealing pressure approaches an asymptotic value as the elastomer and the solvent approach a state of equilibrium.

Swelling involves two concurrent processes such as: the deformation of the network and the migration of the solvent. This section presents in the cylindrical coordinates the governing equations based on a nonlinear field theory of swelling elastomers.[13–23] The essential ingredients of the theory originated from the thermodynamic analysis of Gibbs,[24] the kinetic analysis of Biot,[25] and the statistical mechanical analysis of Flory and Rehner.[26]

We begin with the deformation of the network, Fig. 1. The dry network is taken to be the state of reference, where an infinitesimal element of the network is identified by its distance R from the center of the tubing. At time t, the same element of the network moves to a position at distance r from the center. The deformed network retains the cylindrical symmetry so that the deformation of the elastomer is fully specified by the function $r(R,t)$. Consider a circle, of perimeter $2\pi R$ in the state of reference, and perimeter $2\pi r$ at time t. The circumferential stretch is

$$\lambda_\theta = r/R. \tag{1}$$

Two nearby elements of the network, at positions R and $R+dR$ in the state of reference, move to positions $r(R,t)$ and $r(R+dR,t)$ at time t. The distance between the two elements is dR in the state of reference, and is $r(R+dR,t)-r(R,t)$ at time t. The radial stretch is

$$\lambda_r = \partial r/\partial R. \tag{2}$$

The swelling of the packer in the axial direction is generally minimal due to imposed constraints. Consequently, the packer is assumed to deform under the plane-strain conditions, with no axial deformation. The axial stretch is

$$\lambda_z = 1. \tag{3}$$

We next consider the migration of the solvent. The concentration of the solvent in the network is a time-dependent field, $C(R,t)$, defined as the number of solvent molecules in an element of the network at time t divided by the volume of the element in the state of reference. The solvent migrates in the network in the radial direction, and the flux of the solvent is a time-dependent field, $J(R,t)$, defined as the number of solvent molecules per unit time crossing an element of the network at time t divided by the area of the element in the state of reference. Consider a thin shell of the network, radii R and $R+dR$ when the network is in the state of reference. Between time t and $t+dt$, the number of solvent molecules in the shell changes by $[C(R,t+dt)-C(R,t)]L(2\pi RdR)$, the number of solvent molecules entering the shell from the inner surface is $2\pi RLJ(R,t)dt$, and the number of solvent molecules exiting the shell from the outer surface is $2\pi(R+dR)LJ(R+dR,t)dt$. The conservation of the number of solvent molecules requires that

$$\frac{\partial C}{\partial t} + \frac{\partial (RJ)}{R\,\partial R} = 0. \tag{4}$$

We will use the true stress, namely, the force exerted on a surface in the current state divided by the area of the surface in the current state. Let $\sigma_r(R,t)$ be the field of the radial stress, $\sigma_\theta(R,t)$ the circumferential stress, and $\sigma_z(R,t)$ the axial stress. The elastomer is in mechanical equilibrium at all times. A balance of the forces exerted on an element of the elastomer leads to the equation of equilibrium

$$\frac{\partial (\lambda_\theta \sigma_r)}{\partial R} + \frac{\lambda_\theta \sigma_r - \lambda_r \sigma_\theta}{R} = 0. \tag{5}$$

The elastomer, however, is not in diffusive equilibrium. The chemical potential of the solvent in the elastomer is a time-dependent field, $\mu(R,t)$. The gradient of the chemical potential drives the solvent to migrate in the elastomer. The flux is taken to be linear in the gradient of the chemical potential

$$J = -\frac{CD}{\lambda_r^2 kT}\frac{\partial \mu}{\partial R}, \tag{6}$$

where D is the diffusivity of the solvent. The stretch λ_r appears in Eq. (6) to account for an effect of deformation on migration.[13]

Consider an element of the network, of unit volume in the state of reference. At time t, the element has imbibed a volume of vC of the solvent, and swells to volume $\lambda_\theta\lambda_r$. Here v is the volume per solvent molecule. The stress is typically so small that the volume of each molecule is commonly taken to be constant. Consequently, the volume of the swollen elastomer equals the sum of the volume of the dry network and the volume of the imbibed solvent, namely,

$$\lambda_r\lambda_\theta = 1 + vC. \tag{7}$$

The thermodynamic state of an element of a swollen elastomer is characterized by stretches of the element, λ_r and λ_θ, and the chemical potential of the solvent in the element, μ. The stretches cause a reduction in the entropy of the network, leading to a contractile stress. The chemical potential of the solvent is taken to be zero in the pure solvent. When the chemical potential of the solvent in the elastomer, μ, differs from that in the pure solvent, the difference causes a hydrostatic pressure, μ/v, which contributes to the osmosis of the elastomer relative to the pure solvent. The other contributors to the osmosis are the entropy of mixing and the enthalpy of mixing. These effects are balanced by the mechanical forces acting on the surfaces of the element. Using the free energy calculated by Flory and Rehner based on statistical mechanics,[26] one writes the equations of state as[13]

$$\sigma_r = \frac{kT}{nv\lambda_r\lambda_\theta}(\lambda_r^2 - 1) + \frac{kT}{v}\left[\log\left(1 - \frac{1}{\lambda_r\lambda_\theta}\right) + \frac{1}{\lambda_r\lambda_\theta} + \frac{\chi}{(\lambda_r\lambda_\theta)^2}\right] - \frac{\mu}{v}, \tag{8}$$

$$\sigma_\theta = \frac{kT}{nv\lambda_r\lambda_\theta}(\lambda_\theta^2 - 1) + \frac{kT}{v}\left[\log\left(1 - \frac{1}{\lambda_r\lambda_\theta}\right) + \frac{1}{\lambda_r\lambda_\theta} + \frac{\chi}{(\lambda_r\lambda_\theta)^2}\right] - \frac{\mu}{v}, \tag{9}$$

$$\sigma_z = \frac{kT}{v}\left[\log\left(1 - \frac{1}{\lambda_r\lambda_\theta}\right) + \frac{1}{\lambda_r\lambda_\theta} + \frac{\chi}{(\lambda_r\lambda_\theta)^2}\right] - \frac{\mu}{v}, \tag{10}$$

where n is the number of monomers per polymer chain of the elastomer, kT is the temperature in the unit of energy, and χ is a dimensionless measure of the enthalpy of mixing. In using the Flory–Rehner free energy, we have assumed that the volume per molecule of the solvent is the same as the volume per monomer of the polymer.

Equations (1)–(5) express kinematics of deformation, conservation of solvent, and balance of mechanical forces. Equation (6) specifies a kinetic model, while Eqs. (7)–(10) specify a thermodynamic model. These models are not intended to describe any particular given material with accuracy. Nonetheless the models do capture, at least approximately, some of the most salient features of swelling elastomers, such as the migration of the solvent, the stretching of the network, and the mixing of the network and the solvent. Consequently, the models are expected to predict trends of the swelling behavior. In the remainder of the paper, we refrain from modifying these models but explore their consequences for packers. The method of solution can be readily applied when material models are modified.

III. SWELLING PRESSURE IN THE STATE OF EQUILIBRIUM

As sketched in Fig. 2, after the elastomer touches the wall of the borehole, as the solvent molecules in the elastomer redistribute, the pressure on the wall builds up, and the system approaches a state of equilibrium. This section calculates the swelling pressure in the state of equilibrium. The wall of the borehole is taken to be permeable to the solvent. When the network equilibrates with the solvent, the chemical potential of the solvent in the elastomer becomes homogeneous, and reaches that of the pure solvent, $\mu=0$. Inserting $\mu=0$ into Eqs. (8)–(10), we obtain the equations of state when the network equilibrates with the pure solvent. The state of equilibrium is characterized by a time-independent field in the elastomer, $r(R)$, with the inner surface fixed by the tubing, $r(A)=A$, and the outer surface blocked by the borehole wall, $r(A+H)=B$. A combination of the equations in Sec. II gives rise to a nonlinear, second-order, ordinary differential equation that governs the function $r(R)$. This differential equation, along with the boundary conditions, is solved by using the commercial software MATLAB.

Figure 3 plots the calculated stretches and stresses in the state of equilibrium. The parameters are set as representative values, $A/B=0.6$, $H/B=0.2$, $n=100$, and $\chi=0.1$. Due to the elasticity of the network, even in the state of equilibrium, the field in the elastomer is inhomogeneous. The circumferential stretch in the elastomer, $\lambda_\theta=r/R$, is set by the tubing at the inner surface, $\lambda_\theta=1$, and is set by the borehole at the outer surface, $\lambda_\theta=B/(A+H)$. While the circumferential stretch λ_θ increases with the radius, the radial stretch λ_r decreases. The elastomer is subject to a field of triaxial stress. In particular, the magnitude of σ_r increases along the radius, and reaches the maximum value at the borehole. We have normalized the stress by kT/v. Note that $kT/v \approx 4$ MPa for representative values $T \approx 350$ K and $v \approx 10^{-27}$ m^3.

When the gap between the wall of the borehole and the exterior surface of the tubing is small compared to the radius of the borehole, or equivalently $A/B \to 1$, the curvature of the cylinder becomes unimportant, and the elastomer is approximated by a thin film constrained on a flat rigid substrate. In this thin-film approximation, when the elastomer touches the wall of the borehole, the stretches are

$$\lambda_r = (B-A)/H, \quad \lambda_\theta = 1, \quad \lambda_z = 1. \tag{11}$$

Inserting these stretches and $\mu=0$ into Eq. (8), we obtain that

$$\frac{\sigma_r}{kT/v} = \frac{1}{n}\left(\lambda_r - \frac{1}{\lambda_r}\right) + \log\left(1 - \frac{1}{\lambda_r}\right) + \frac{1}{\lambda_r} + \frac{\chi}{\lambda_r^2}. \tag{12}$$

This expression is the thin-film approximation of the radial stress in the state of equilibrium.

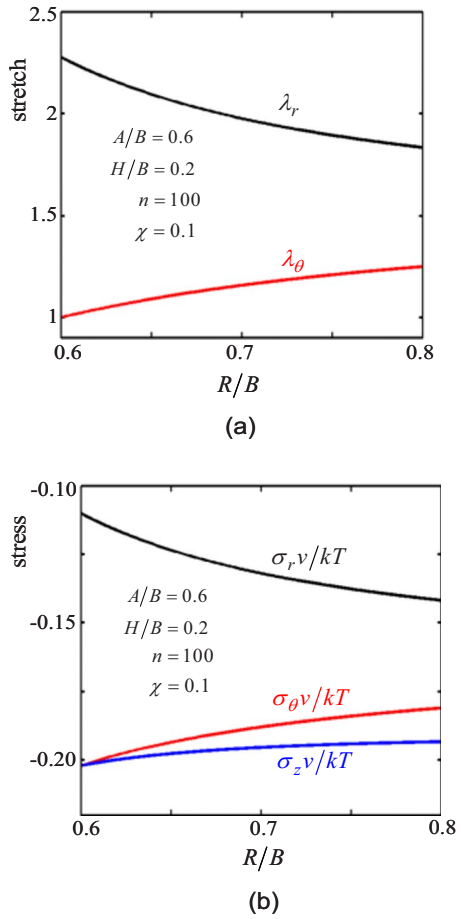

FIG. 3. (Color online) In the elastomer, even when the distribution of the solvent reaches a state of equilibrium, the stretches (a) and the stresses (b) are still inhomogeneous.

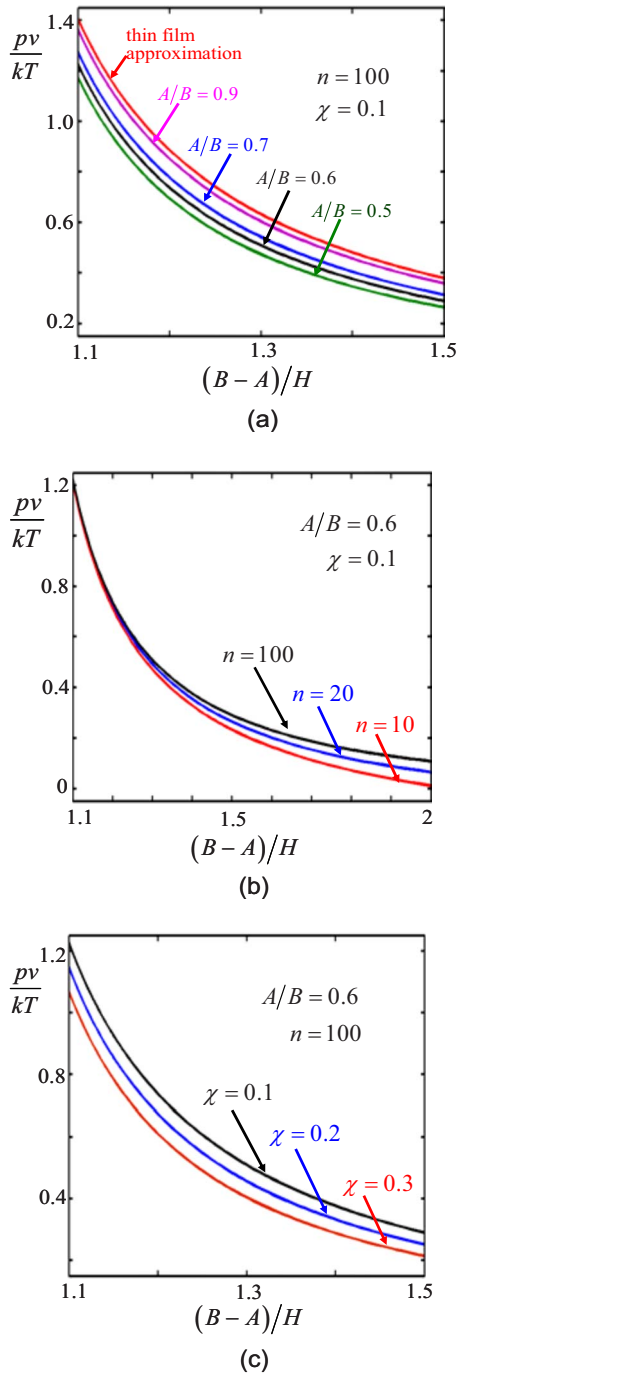

FIG. 4. (Color online) The sealing pressure is plotted as a function of the ratio $(B-A)/H$. (a) The effect of the ratio of the radius of the tubing over that of the borehole, A/B. (b) The effect of the number of monomers per polymer chain, n. (c) The effect of the affinity between the polymer and the solvent, χ.

As shown in Fig. 3, in general, the stretches are inhomogeneous in the elastomer, and $\lambda_r \neq (B-A)/H$. Nonetheless, we can still use the ratio $(B-A)/H$ as a dimensionless measure of the deformation needed to close the gap between the borehole wall and the elastomer. The sealing pressure in the state of equilibrium, $p=-\sigma_r(A+H)$, is perhaps one of the most important parameters for a packer. Figure 4 plots the sealing pressure as a function of $(B-A)/H$. Everything else being the same, the sealing pressure decreases when $(B-A)/H$ decreases. Also included in Fig. 4(a) is the thin-film approximation (12). As expected, this approximation becomes accurate when $A/B \to 1$.

In addition to these geometric factors, the nature of the network and solvent also affects the sealing pressure. When the number of monomers per polymer chain, n, increases, the contractile stress of the network decreases so that the sealing pressure increases, Fig. 4(b). This effect is appreciable when the elastomer has to swell much to close the gap, namely, when $(B-A)/H$ is large. When the affinity between the polymer and the solvent is low (i.e., large and positive χ), the sealing pressure is small.

IV. KINETIC PROCESS AND SWELLING TIME

As illustrated in Fig. 2, the kinetic process may be divided into two stages, before and after the elastomer touching the borehole wall. The basic equations in Sec. II can be combined to evolve the two time-dependent fields, $r(R,t)$ and $\mu(R,t)$. At the inner surface, $R=A$, the position is fixed by the tubing, $r=A$, and the flux vanishes, $\partial\mu/\partial R=0$. At the outer surface, $R=A+H$, before the elastomer touches the borehole wall, the redial stress vanishes, $\sigma_r=0$, and the solvent molecules in the elastomer are in equilibrium with those in the pure solvent outside, $\mu=0$. After the elastomer touches the borehole wall, the boundary conditions at the outer surface become that the position is set by the borehole, $r=B$,

and the chemical potential remains, $\mu=0$. The latter boundary condition in effect assumes that the borehole wall is permeable to the solvent.

In the Flory–Rehner theory, [Eqs. (8)–(10)], when the network is immersed in the solvent, the stress becomes singular if the elastomer contains no solvent, $\lambda_r=\lambda_\theta=\lambda_z=1$. To avoid this singularity in calculation, we assume that at time $t=0$ the elastomer already contains a small amount of solvent, in a homogeneous state of chemical potential, $\mu(R,0)=\mu_0$. The elastomer is assumed to be in a state of equilibrium, so that the initial radial position $r(R,0)$ can be calculated by solving the ordinary equation in Sec. III, with the boundary conditions $r(A)=A$ and $\sigma_r(A+H)=0$. The initial chemical potential is set as $\mu_0<0$, and the exact value does not affect the finial sealing pressure significantly, so long as μ_0 corresponds to a small concentration of solvent. These initial conditions, along with the boundary conditions discussed above, are used to solve the partial differential equations in Sec. II by using the finite-difference method. We normalize the time as Dt/H^2.

Consider a representative case with $A/B=0.6$, $H/B=0.2$, $n=100$, and $\chi=0.1$. Figure 5(a) plots the profile of the radial position at several times. At all times, the inner surface is fixed by the metallic tubing, $r(A,t)=A$. The outer surface move with time before the elastomer touches the borehole wall. Upon touching the borehole, $Dt/H^2\approx 5$, the outer surface of the elastomer is fixed by the borehole wall, $r(A+H,t)=B$. Because individual molecules are assumed to maintain constant volumes, no more solvent molecules can enter the elastomer after it touches the wall of the borehole. The elastomer, however, is not in equilibrium with the solvent, and the solvent molecules inside the elastomer keep redistributing. This redistribution accounts for the continued evolution of the profile of the radial position.

Figure 5(b) plots the distribution of the chemical potential of the solvent in the elastomer at several times. Prior to immersion, the chemical potential of solvent in the elastomer is homogeneous and is assumed to be at a low level μ_0. At the instant of immersion, the chemical potential at the outer surface immediately rises to the value of the pure solvent, $\mu(A,t)=0$, and is held at this value by the external solvent afterwards. As time progresses, the chemical potential rises in the interior of the elastomer. When the elastomer touches the borehole, $Dt/H^2\approx 5$, the solvent molecules in the elastomer are still not equilibrated. After a long time, the chemical potential becomes homogeneous, and is at the same level as the external solvent $\mu=0$. That is, the elastomer equilibrates with the solvent.

Figure 5(c) plots the profile of concentration of solvent at several times. At the instant of immersion, the concentration of solvent at the outer surface jumps to a high value. As the time progresses, the concentration in the interior also rises. After the elastomer touches the borehole, no more solvent enters the elastomer but the solvent inside the elastomer redistributes. After a long time, the profile of concentration stops evolving, and the elastomer reaches the state of equilibrium. Even in the state of the equilibrium, the concentration of the solvent in the elastomer is inhomogeneous [the inset of Fig. 5(c)]. Recall that the condition of diffusive equilibrium is set by homogenizing the chemical potential, not by homogenizing the concentration. In this particular case, the inhomogeneity of the concentration in the state of equilibrium is not pronounced. However, pronounced inhomogeneity in the concentration of the solvent in the state of equilibrium was noted in a spherical core-shell structure.[14]

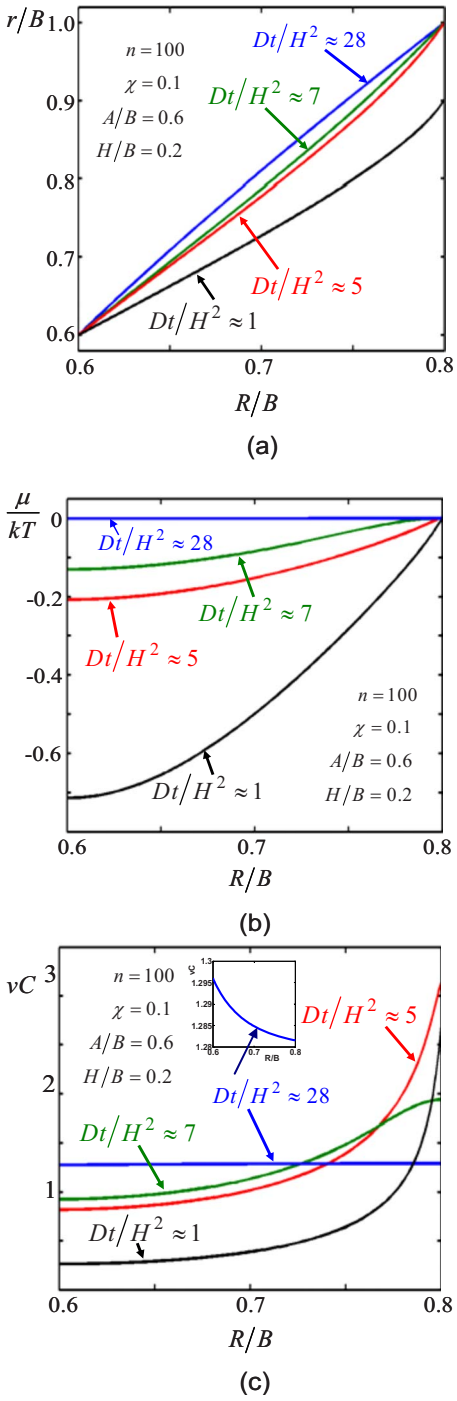

FIG. 5. (Color online) Evolution of the fields of (a) the normalized radial position, (b) the chemical potential of the solvent, and (c) the concentration of the solvent. The inset in (c) shows that the concentration of the solvent in the elastomer remains inhomogeneous even as the state of equilibrium is approached.

Figure 6 plots the pressure exerted by the elastomer on the wall of the borehole as a function of time. In each case, the elastomer approaches a state of equilibrium after a long

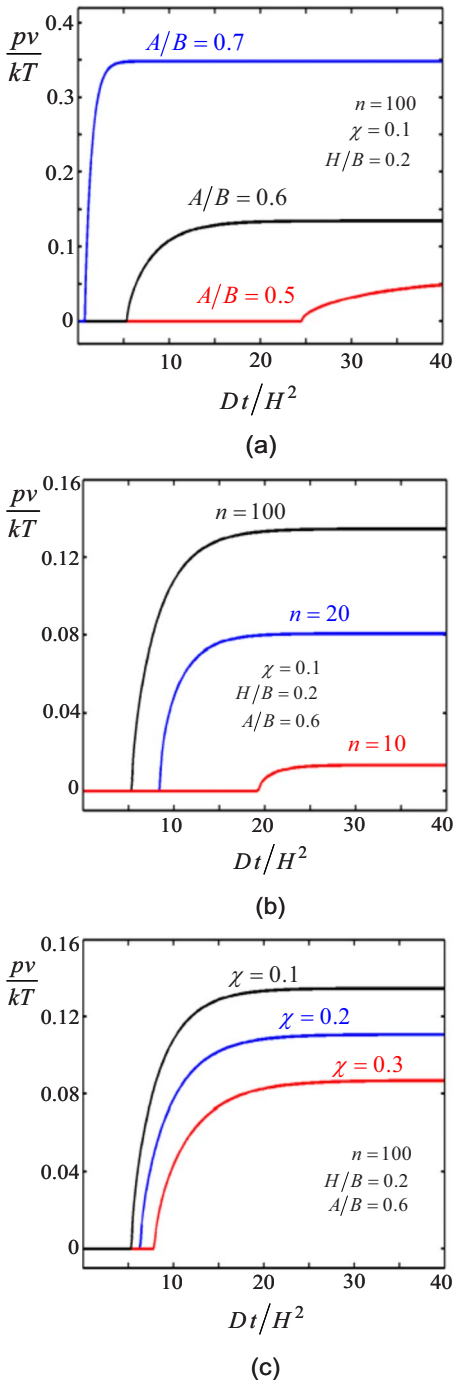

FIG. 6. (Color online) The sealing pressure as a function of time. (a) The effect of the ratio of the radius of the tubing over that of the borehole, A/B. (b) The effect of the number of monomers per polymer chain, n. (c) The effect of the affinity between the polymer and the solvent, χ.

time. The asymptotic values of the sealing pressure have been discussed in Sec. II. We now focus on the times needed for the pressure to attain the asymptotic values. After the elastomer touches the wall of the borehole, no more solvent molecules enter the elastomer. The solvent molecules inside the elastomer, however, take substantial time to redistribute for the stealing pressure to attain the asymptotic value. Indeed, the time needed for redistribution is comparable to the time needed for the elastomer to touch the wall of the borehole. Various dimensionless parameters affect the sealing time. Our calculation shows that when a parameter increases the asymptote of the sealing pressure, the parameter also shortens the time needed to attain the asymptote.

V. CONCLUDING REMARKS

A swelling packer involves concurrent deformation and migration, governed by a nonlinear field theory. The sealing pressure is affected by the geometry of the constraint, the chain length of the polymer, and the affinity between the polymer and the solvent. The sealing time includes both the time needed for the elastomer to swell to touch the wall of the borehole, and the time for the pressure to build up to the state of equilibrium. The calculations are based on the equations of state derived from the Flory–Rehner model, and on a kinetic model that account for the effect of deformation on migration. While these material models relate the behavior of a packer to the nature of the network and solvent, the accuracy of these models need be tested against experimental data.

ACKNOWLEDGMENTS

The work at Harvard University is supported by the National Science Foundation through a Grant No. CMMI-0800161, by Schlumberger through a gift and by the Kavli Institute.

[1]M. F. Refojo, in *Biomaterials Science*, edited by B. D. Ratner, A. S. Hoffman, F. J. Schoen, and J. E. Lemons (Elsevier, Boston, 2004), pp. 583–590.
[2]F. Masuda, in *Superabsorbent Polymers*, edited by F. L. Buchholtz and N. A. Peppas (American Chemical Society, Washington, D.C., 1994), pp. 88–98.
[3]M. A. Zwieniecki, P. J. Melcher, and N. M. Holbrook, Science **291**, 1059 (2001).
[4]D. J. Beebe, J. S. Moore, J. M. Bauer, Q. Yu, R. H. Liu, C. Devadoss, and B. H. Jo, Nature (London) **404**, 588 (2000).
[5]K. W. Oh and C. H. Ahn, J. Micromech. Microeng. **16**, R13 (2006).
[6]P. Cavanagh, C. R. Johnson, S. LeRoy-Delage, G. DeBrujin, I. Cooper, D. Guillot, H. Bulte, and B. Dargaud, SPE/IADC Drilling Conference, Amsterdam, Netherlands, 20–22 February, 2007 (Society of Petroleum Engineers, Richardson, TX, 2007).
[7]N. Moroni, N. Panciera, A. Zanchi, C. R. Johnson, S. LeRoy-Delage, H. Bulte-Loyer, S. Cantini, and E. Belleggia, SPE Annual Technical Conference and Exhibition, Anaheim, California, USA, 11–14 November, 2007..
[8]J. Roth, C. Reeves, C. R. Johnson, G. De Bruijn, M. Bellalarba, S. LeRoy-Delage, and H. Bulte-Loyer, IADC/SPE Drilling Conference, Orlando, Florida, USA, 4–6 March, 2008 (Society of Petroleum Engineers, Richardson, TX, 2008).
[9]M. Kleverlaan, R. H. van Noort, and I. Jones, SPE/IADC Drilling Conference, Amsterdam, Netherlands, 23–25 February, 2005 (Society of Petroleum Engineers, Richardson, TX, 2005).
[10]V. Fjellatad, R. Berbkvam, and T. Li, Hart's E&P (79), 79–81, October 2006 http://www.epmag.com/archives/features/6276.htm
[11]M. S. Laws, J. E. Fraser, H. F. Soek, and N. Carter, Asia Pacific Drilling Conference and Exhibition, Bangkok, Thailand, 13–15 November, 2006.
[12]D. Hembling, S. Salamy, A. Qatani, N. Carter, S. Jacob, Drilling Contractor, 108–114, September/October, 2007.
[13]W. Hong, X. H. Zhao, J. X. Zhou, and Z. G. Suo, J. Mech. Phys. Solids **56**, 1779 (2008).
[14]X. H. Zhao, W. Hong, and Z. G. Suo, Appl. Phys. Lett. **92**, 051904 (2008).
[15]W. Hong, Z. S. Liu, and Z. G. Suo, Int. J. Solids Struct. **46**, 3282 (2009).
[16]J. P. Zhang, X. H. Zhao, Z. G. Suo, and H. Q. Jiang, J. Appl. Phys. **105**, 093522 (2009).
[17]S. S. Sternstein, J. Macromol. Sci., Phys. **B6**, 243 (1972).
[18]K. Sekimoto, J. Phys. II **1**, 19 (1991).

[19]S. Govindjee and J. C. Simo, J. Mech. Phys. Solids **41**, 863 (1993).
[20]C. J. Durning and K. N. Morman, J. Chem. Phys. **98**, 4275 (1993).
[21]S. Baek and A. R. Srinivasa, Int. J. Non-linear Mech. **39**, 1301 (2004).
[22]J. Dolbow, E. Fried, and H. D. Jia, J. Mech. Phys. Solids **52**, 51 (2004).
[23]H. Li, R. Luo, E. Birgersson, and K. Y. Lam, J. Appl. Phys. **101**, 114905 (2007).
[24]J. W. Gibbs, The Scientific Papers of J. Willard Gibbs (Digital copy of the book is available at http://books.google.com/), pp. 184, 201, 215, 1878.
[25]M. A. Biot, J. Appl. Phys. **12**, 155 (1941).
[26]P. J. Flory and J. Rehner, J. Chem. Phys. **11**, 521 (1943).